

Characterization of the NEP of Mid-Infrared Upconversion Detectors

Rasmus Lyngbye Pedersen[✉], Lasse Høgstedt, Ajanta Barh, Lichun Meng, and Peter Tidemand-Lichtenberg[✉]

Abstract—We present a scheme to estimate the noise equivalent power (NEP) of the frequency upconversion detectors (UCDs), detecting mid-infrared (MIR) light. The NEP of the UCD is a combined contribution of NEPs from the upconversion process and from the photodetector, used for detecting the upconverted signal. The 2–5-μm MIR range is particularly investigated in this letter using a bulk periodically poled lithium niobate-based CW-intracavity UCD. We measured the NEP of UCD as $20 \text{ fW}/\sqrt{\text{Hz}}$ at the MIR wavelength of 3.39 μm. Here, we showed that the limiting factor is not the noise from the upconversion process (estimated NEP is $2.3 \text{ fW}/\sqrt{\text{Hz}}$ at 3.39 μm) but from the electrical noise in the photodetector itself. We also compared the performance of our UCD with the previously published results and with market available direct MIR detectors. In addition, we measured the optical noise of the UCD over its working spectral range (2.9–3.6 μm) and compared with the numerical simulation.

Index Terms—Infrared detectors, noise, nonlinear optical devices, sensor systems and applications.

I. INTRODUCTION

FOR a number of applications, spectroscopy in the mid-infrared (MIR: 2 - 10 μm) spectral range is desirable. Several molecules and materials have distinct and strong absorption/emission features in the MIR due to the rotational-vibrational transitions of the molecular bonds. For instance, in the field of combustion research, molecules of particular interest with MIR-features are: sulfate compounds (SO_2 , CS_2 , H_2S , OCS), hydrogen halides (HCl and HF), small hydrocarbons (CH_4 , C_2H_2 , C_2H_4 , C_2H_5), toxic species like HCN, and hydrocarbon radicals (e.g. CH_3). To detect these substances with high sensitivity, good light sources and detectors are needed. In the last decades MIR sources have seen much improvement with advances made to quantum cascade lasers, optical parametric oscillators and fiber lasers, both for narrow linewidth applications and for broadband-high brightness sources. In contrary, the development of detectors have struggled by the inherent thermal noise in low bandgap materials

Manuscript received December 19, 2018; revised February 15, 2019; accepted February 21, 2019. Date of publication March 12, 2019; date of current version April 22, 2019. This work was supported in part by Mid-TECHH2020-MSCA-ITN-2014 under Grant 642661. (Corresponding author: Rasmus Lyngbye Pedersen.)

R. L. Pedersen is with Lund University, SE-221 00 Lund, Sweden (e-mail: rasmus.lyngbye_pedersen@forbf.lth.se).

L. Høgstedt is with NLIR Asp., 3520 Farum, Denmark.

A. Barh, L. Meng, and P. Tidemand-Lichtenberg are with DTU Fotonik, 4000 Roskilde, Denmark.

Color versions of one or more of the figures in this letter are available online at <http://ieeexplore.ieee.org>.

Digital Object Identifier 10.1109/LPT.2019.2904325

(PbS, PbSe, HgCdTe), and because there is a significant amount of thermal radiation in the MIR from the environment at room temperature. These limitations have been circumvented by using parametric frequency upconversion to move the MIR signal to the visible or near infrared (NIR) range [1]. This technique has seen rapid development within the last decade. It has been shown to have low noise and work well with spectroscopic methods used in, for instance, combustion physics [2], [3]. However, depending on the wavelength of detection and the nonlinear material, upconversion cannot remove the environmental thermal noise completely [4], and the spectral or temporal noise of the mixing laser will be added to the signal [5]. Previously, NEP of around $1 \times 10^{-17} \text{ fW}/\sqrt{\text{Hz}}$ have been measured for upconversion detector working in CW [6], and for pulsed [7] NIR systems. In both cases [6], [7], the upconversion is realized using nonlinear waveguides based on a single pass configuration. Hence it is not directly comparable to the work presented here. In this article, we characterize the overall noise performance of a CW intracavity based upconversion detector using a bulk nonlinear crystal in the 2 - 5 μm range.

II. THEORY

Upconversion is realized by mixing MIR signal photons at frequency ω_{IR} with pump photons at frequency ω_p to generate VIS/NIR upconverted photons at frequency ω_{up} , when satisfying the conservation of energy ($\omega_{IR} + \omega_p = \omega_{up}$). This letter is particularly targeting the 2 - 5 μm MIR spectral range for gas species detection, and will focus on periodically poled lithium niobate (PPLN) [8] as the nonlinear mixing crystal. To yield the highest conversion efficiency, the quasi-phase matching (QPM) condition should be satisfied [9] as follows: $k_{up} - k_{IR} - k_p - 2\pi/\Lambda = 0$, where, k_{up} , k_{IR} , and k_p are the wavevectors of the upconverted (up) light, MIR (IR) signal, and the pump (p), respectively, and Λ is the poling period of the PPLN. To characterize the NEP of an upconversion detector, it is important to consider both the upconversion quantum efficiency (η_{up}) [10] and the optical noise generated in the upconversion module. In the following we briefly discuss the sources of optical noises and give a recipe to calculate the NEP.

A. Optical Noise Originating From the Upconversion

To our best knowledge, the two primary noise sources in a PPLN upconversion module are upconverted thermal [4] and

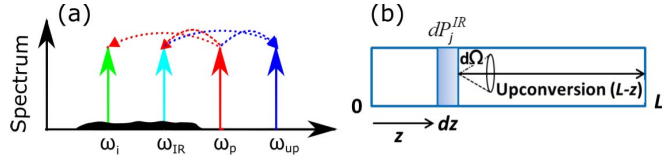


Fig. 1. (a) Schematic spectrum of generated SPDC (red → green + cyan) followed by the upconversion process (cyan + red → blue). The black curve represents the broadband nature of generated SPDC. Noted, ω_i can also be larger than ω_{IR} . (b) Infrared radiation originated inside the PPLN generates the upconverted noise along the length.

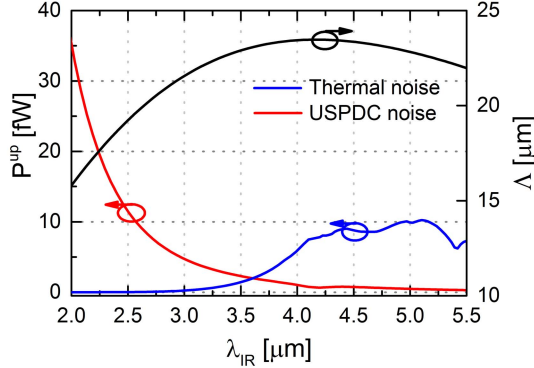


Fig. 2. Calculated upconverted thermal (blue curve), USPDC noise (red curve) and poling period (black curve) as a function of λ_{IR} . In the calculation, $\lambda_P = 1064 \text{ nm}$, operation temperature $T = 17^\circ\text{C}$, beam waist of 1064 nm pump is $80 \mu\text{m}$, pump power is 80 W, central wavelength of the bandpass filter is assumed to have the same value as the upconverted signal and $\Delta\lambda_{FWHM} = 2 \text{ nm}$, the poling error $\sigma = 0.5 \text{ nm}$.

spontaneous parametric downconversion (SPDC) noise [11]. According to Kirchhoff's radiation law, the PPLN generates thermal radiation in the $2 - 5 \mu\text{m}$ range, emitted in all direction, due to its finite temperature and absorption coefficient. Similarly, the pedestal effect caused by the random duty cycle (RDC) error can enhance the non-phase-matched process [11], which results in generation of broadband SPDC photons, see Fig. 1(a). The part of infrared radiation (thermal and SPDC) that satisfies the phase matching condition for the upconversion process, contributes to the optical noise.

The two noise terms can be treated similarly. dP_j^{IR} is the infrared radiation power from a slab of thickness dz inside the PPLN over a solid angle $d\Omega$, where j can be thermal (th) or SPDC ($SPDC$), see Fig. 1(b). The associated upconverted power P_j^{up} is found by the integral:

$$P_j^{up}(\lambda_{IR}, p_j) = B_j \int dP_j^{IR}(\lambda_{IR}, p_j) \eta_{up}(L-z, \lambda_{IR}, \Omega) dz d\Omega \quad (1)$$

The pre-factor B_j originates from the upconversion of the thermal radiation/SPDC process. p_j is parameters of the two processes, where $p_{th} = T$ (temperature of PPLN) and $p_{SPDC} = \sigma$ (RDC error). The λ_{IR} is the wavelength of the infrared noise (thermal and SPDC). The total upconverted noise power is $P_N = P_{th}^{up} + P_{SPDC}^{up}$.

Using Eq. 1, we have estimated the power of the aforementioned noise sources over the $2 - 5 \mu\text{m}$ range, see Fig. 2. The upconverted SPDC is the main noise source in the lower

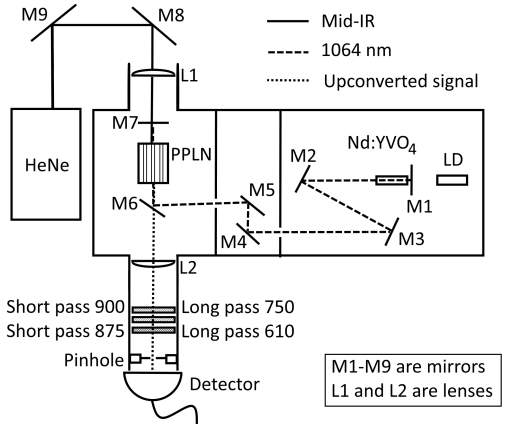


Fig. 3. Mirrors M1-M7 are HR coated for 1064. M1-M5 are transmissive for 808 nm and M6 and M7 are transmissive for the upconverted and the IR signal, respectively.

spectral range since the non-phase-matched SPDC process has higher pedestal level in this region (see [12, Fig. 3]). The upconverted thermal noise is dominating above $3 \mu\text{m}$ resulting from the linear absorption in the crystal [13].

B. Noise Equivalent Power (NEP)

Based on the discussion in the previous section, the average power of the background noise P_N due to upconverted SPDC and thermal radiation can be calculated theoretically. The performance of the photodetector, used to detect the upconverted signal, should also be considered when evaluating the performance of the upconversion detector (upconversion module + photodetector). The parameter, NEP, is widely used to characterize the sensitivity of detectors. In this section, we calculate the NEP of the upconversion detector theoretically.

Assuming a photodetector is used for the detection of the upconverted signal, the SNR of the upconversion detector is

$$\text{SNR} = \frac{i_s}{\sqrt{\sigma_N^2 + \sigma_{det}^2}}, \quad (2)$$

where $i_s = P_{IR} \eta_{up} \eta_{det} q / \hbar \omega_{IR}$ is the current driven by the input signal to the detector, q is the electron charge. $\sigma_N = \sqrt{2qBM^2F(i_s + i_n)}$ is the shot noise driven by the current, F is the excess noise factor of the photodetector, M is the gain [14], and $i_n = P_N \eta_{det} q / \hbar \omega_{up}$ is the current driven by the optical noise. Note, the noise photon is assumed to have the same angular frequency as the unconverted signal. σ_{det} is the noise of the photodetector, and it can be approximated as $\text{NEP}_{det} \eta_{det} q \sqrt{B / \hbar \omega_{up}}$, where NEP_{det} is the NEP of the photodetector. Thus, the NEP of the upconversion detector can be calculated by equating $\text{SNR} = 1$, which gives

$$\text{NEP} = \frac{\omega_{IR}}{\omega_{up} \eta_{up}} \sqrt{\frac{2FM^2 P_N \hbar \omega_{up}}{\eta_{det}}} + \text{NEP}_{det}^2. \quad (3)$$

It is necessary to emphasize that the shot noise introduced by i_s is neglected here by assuming it is smaller than the other noise sources. Based on equation 3, the noise source can be separated into two parts: upconversion noise and the photodetector noise. A new parameter can be defined as

$P_{critical} = NEP_{det}^2 \eta_{det} / (2M^2 F \hbar \omega_{up})$. When $P_N > P_{critical}$, the performance of the system can be improved using noise reduction strategies, e.g. narrow spectral filtering, spatial filtering, and choosing proper poling period. In contrast, when $P_N < P_{critical}$, the photodetector becomes the bottleneck of the upconversion detector, and the performance of the upconversion detector cannot be improved significantly by simply reducing the P_N .

In practice, the NEP can be calculated based on the output of the photodetector directly [15]:

$$NEP = \frac{\sigma_b}{p_r \sqrt{B}}, \quad (4)$$

where σ_b is the standard deviation of the output of the photodetector and p_r is the power response of the detector, which can be calculated as $p_r = (\bar{x}_s - \bar{x}_b) / P_{opt}$, where P_{opt} is the optical input power of the upconversion detector, and \bar{x}_s and \bar{x}_b are the average outputs of the photodetector with and without input signal, respectively.

III. EXPERIMENTAL SETUP

Fig. 3 shows the diagram of the experimental setup. A 4 mW continuous wave HeNe laser with a wavelength of 3.39 μm was used as the MIR signal. The HeNe beam is guided by M8 and M9 and then focused by L1 ($f = 75$ mm, germanium lens) into the PPLN crystal forming a beam waist of 89 μm , to match the 1064 nm pump beam waist (90 μm). The HeNe beam is aligned to optimize the overlap between the two beams inside the PPLN. The PPLN was 25 mm long with 10 different poling period channels. The cavity of the 1064 nm laser consists of mirrors M1-M7. The laser crystal is an Nd:YVO₄, pumped by a 4 W, 808 nm laser diode (LD). The laser cavity is built with several baffles and mirrors (M2-M5), to remove the remainder of the LD light. The PPLN crystal is between mirrors M6 and M7, and its temperature is controlled by an oven. The upconverted signal is collimated with the lens L2 ($f = 60$ mm). A pinhole, 700 μm in diameter, is used to remove the non-collinear upconverted thermal radiation. The filter set shown in Figure 3 is used to remove the 1064 nm laser leaking from the cavity, and the 532 nm second harmonic generated in the PPLN. A Thorlabs PDF10A photodetector is used to measure the upconverted signal. To avoid saturation of the detector, ND filters are added in front of L1 to reduce the signal. The photodetector is connected to a Tektronix TDS 1002 oscilloscope.

IV. RESULTS AND DISCUSSION

Before determining the optical noise contribution from the upconversion module, the electronic noise contributions from the oscilloscope (osc.) and the photodetector (PD) is characterized by measuring the readout of the osc. over 1 second, with 1 ms time resolution for three cases, see Table I. The noise contribution from the upconversion module is negligible compared with the noise from the PD.

To determine the power response, a known power input of 0.25 pW was generated by reducing the 4.0 mW HeNe laser beam with ND filters calibrated to ND10.2. The signal generated with this input was 34.4 mV, corresponding to a power response of $1.35 \times 10^{11} \text{ V/W}$. Combining the power

TABLE I
ELECTRIC NOISE*

Noise source	Osc.	Osc. and PD	Osc., PD and Upc.
Mean (mV)	0.2	19	85
STD (mV)	0.26	8.5	8.6

* In this measurement, the PPLN poling period is 22.7 μm and the crystal is at 17 $^\circ\text{C}$.

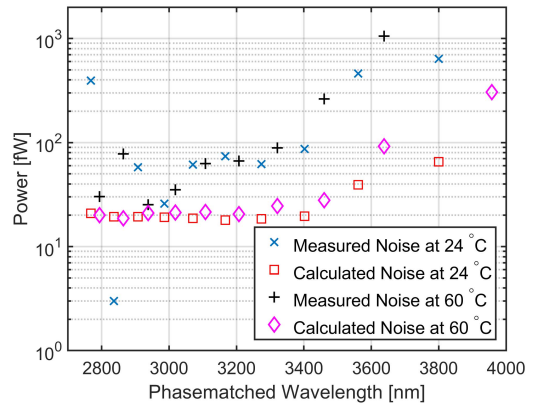


Fig. 4. Comparison of measured and calculated noise powers as a function of wavelength with the PPLN at 24 $^\circ\text{C}$ and 60 $^\circ\text{C}$.

response with the background STD in Eq. 4 gives a NEP of $20 \text{ fW}/\sqrt{\text{Hz}}$. If the noise contribution from the upconversion module is negligible, it can be seen from Eq. 3 that the NEP is the NEP of the detector scaled by the conversion efficiency of the upconverter. While this is the case, increasing the conversion efficiency will lower the NEP, while simultaneously increasing the generated optical noise, until the detector is no longer the limiting factor.

The upconversion detector is capable of phase-matching over a wide wavelength range, and the noise power depends on the phase-match condition. In Fig. 4 the measured noise power is shown for different poling periods and compared with the noise power calculated using Eq. 1. There are a few outliers, that do not follow the trend predicted by the calculations. This could be a result of imperfect alignment, as the phase-match could only be optimized at 3.39 μm , before translating the PPLN to a different poling period channel. Alternatively, it might be an effect of different errors in the poling period of each channel. The measured noise power are on average five times larger than the calculated values, but follows the trend suggested by the calculations. The measured noise power depends on the poling period and crystal temperature, which suggests that the source of the additional noise is not stray light from the LD pump. It is at this point unclear what the source of the additional noise is.

As discussed above, the electronic noise in the detector dominates the overall noise. Determining the noise limit set by the noise generated in the upconversion module alone would make it possible to choose a detector that does not further limit detection sensitivity. Assuming the background photon noise is Poisson distributed, an estimated NEP reachable with a better detector can be calculated. For a Poisson distribution, the STD is the square root of the mean number of events. Assuming photon noise level of 500 fW as a rough value, or $2.0 \cdot 10^6$ photons at 810 nm, the STD is $\sigma = 1.4 \cdot 10^3$ photons

TABLE II
NEP COMPARISON OF DETECTORS

Detector	Bandwidth [Hz]	NEP* [pW/ $\sqrt{\text{Hz}}$]	NEP upc.** [pW/ $\sqrt{\text{Hz}}$]	η_{up}	η_{total}
PDF10A+UpC	20	$1.4 \cdot 10^{-3}$	$2.0 \cdot 10^{-2}$	6.0%	2.0 %
Vigo PVI-4TE-5-1x1	$55 \cdot 10^6$	1.0	NA	NA	66%
Teledyne 0.1 mm	$50 \cdot 10^6$	$80 \cdot 10^{-3}$	NA	NA	55%
Hamamatsu+UpC***	$1 \cdot 10^9$	$1.5 \cdot 10^{-3}$	75	$3.6 \cdot 10^{-6}$	$2.7 \cdot 10^{-6}$
Perkin-Elmer+UpC***	$7 \cdot 10^9$	$0.86 \cdot 10^{-3}$	43	$3.6 \cdot 10^{-6}$	$2.7 \cdot 10^{-6}$
SPC+UpC****	NA	$1.3 \cdot 10^{-5}$	$2.6 \cdot 10^{-5}$	32.9%	10.5%

* The NEP of the photodetector.

** The NEP for upconversion detector (photodetector + upconversion module).

*** The results are reproduced from [16].

**** The results are reproduced from [17], SPC stands for single photon counter. A pulsed laser is used as the pump in [17], NEP upc., η_{up} and η_{total} are the instantaneous values when the pump is at the peak power.

per second. For an integration time of 1 s, the NEP can be calculated by:

$$\text{NEP} = \frac{\sigma E_p \omega_{IR}}{\omega_{up} \eta_{up} \sqrt{\Delta f}} = 2.3 \text{ fW}/\sqrt{\text{Hz}} \quad (5)$$

where E_p is the energy per photon, $\eta_{up} = 6.0\%$ and Δf is 0.5 Hz. For the contribution of the detector noise to negligible, NEP_{det} should be much smaller than the value above. If the detector noise is the dominant noise source, the NEP of the upconversion detector can be estimated as $\omega_{IR}/(\omega_{up} \eta_{up})\text{NEP}_{det}$.

V. COMPARISON WITH OTHER MIR DETECTORS

In Table II the NEP determined in this article is compared with two MIR detectors, and previous results using upconversion. The MIR detector examples chosen are market available cutting edge direct MIR detectors, a Vigo photodiode as an example of MIR detector with cryogenic cooling (-78°C), and an InSb photodiode from Teledyne as an example of a liquid nitrogen cooled detector. The combination of the PDF10A photodiode and upconversion (working temperature $\approx 20^\circ\text{C}$) compare favorably with direct detection in terms of NEP. When comparing with the work by Zhou *et al.* [17], the pure value for the reported NEP is almost three orders of magnitude better than the figure presented here. However, the upconversion pump in the system described in [17] is pulsed, and the NEP and conversion efficiency calculated only for the duration of the pulse. Their upconversion pump laser pulse duration is 5.3 ps, at 17.9 MHz repetition rate, giving a duty cycle of only 0.01 %. With a similar time gating, our noise would decrease four orders of magnitude. When comparing with previous CW upconversion results from [16], it can be seen that the NEP has been improved by almost 3 order of magnitude, while using a detector with a higher NEP. This is a result of the higher η_{up} reached here.

ACKNOWLEDGEMENT

The authors would like to thank the company NLIR Apps for making equipment and space available for this work.

REFERENCES

- [1] J. S. Dam, P. Tidemand-Lichtenberg, and C. Pedersen, "Room-temperature mid-infrared single-photon spectral imaging," *Nature Photon.*, vol. 6, no. 11, pp. 788–793, Sep. 2012.
- [2] L. Høgstedt *et al.*, "Low-noise mid-IR upconversion detector for improved IR-degenerate four-wave mixing gas sensing," *Opt. Lett.*, vol. 39, no. 18, pp. 5321–5324, Sep. 2014.
- [3] R. L. Pedersen, D. Hot, and Z. S. Li, "Comparison of an InSb detector and upconversion detector for infrared polarization spectroscopy," *Appl. Spectrosc.*, vol. 72, no. 5, pp. 793–797, May 2018.
- [4] A. Barh, P. Tidemand-Lichtenberg, and C. Pedersen, "Thermal noise in mid-infrared broadband upconversion detectors," *Opt. Express*, vol. 26, no. 3, pp. 3249–3259, Feb. 2018.
- [5] L. Meng, L. Høgstedt, P. Tidemand-Lichtenberg, C. Pedersen, and P. J. Rodrigo, "GHz-bandwidth upconversion detector using a unidirectional ring cavity to reduce multilongitudinal mode pump effects," *Opt. Express*, vol. 25, no. 13, pp. 14783–14794, Jun. 2017. doi: 10.1364/OE.25.014783.
- [6] J. S. Pelc *et al.*, "Long-wavelength-pumped upconversion single-photon detector at 1550 nm: Performance and noise analysis," *Opt. Express*, vol. 19, no. 22, pp. 21445–21456, Oct. 2011.
- [7] H. Dong, H. Pan, Y. Li, E. Wu, and H. Zeng, "Efficient single-photon frequency upconversion at 1.06 μm with ultralow background counts," *Appl. Phys. Lett.*, vol. 93, no. 7, Aug. 2008, Art no. 071101.
- [8] A. Barh, C. Pedersen, and P. Tidemand-Lichtenberg, "Ultra-broadband mid-wave-IR upconversion detection," *Opt. Lett.*, vol. 42, no. 8, pp. 1504–1507, Apr. 2017.
- [9] B. E. A. Saleh and M. C. Teich, "Nonlinear optics," in *Fundamentals Photons*, 2nd ed. Hoboken, NJ, USA: Wiley, 2007, ch. 21, sec. 2, pp. 879–894.
- [10] R. L. Sutherland, "Frequency doubling and mixing," in *Handbook Nonlinear Optical*, 2nd ed. New York, NY, USA: MARDEK, 2003, ch. 2, pp. 83–88.
- [11] J. S. Pelc, C. R. Phillips, D. Chang, C. Langrock, and M. M. Fejer, "Efficiency pedestal in quasi-phase-matching devices with random duty-cycle errors," *Opt. Lett.*, vol. 36., no. 6, pp. 864–866, Mar. 2011.
- [12] C. R. Phillips, J. S. Pelc, and M. M. Fejer, "Parametric processes in quasi-phased matching gratings with random duty cycle errors," *J. Opt. Soc. Amer. B, Opt. Phys.*, vol. 30, no. 4, pp. 982–993, 2013.
- [13] M. Leidinger, S. Fieberg, N. Waasem, F. Kühnemann, K. Buse, and I. Breunig, "Comparative study on three highly sensitive absorption measurement techniques characterizing lithium niobate over its entire transparent spectral range," *Opt. Express*, vol. 23, pp. 21690–21705, Aug. 2015.
- [14] J. Zheng *et al.*, "Digital alloy InAlAs avalanche photodiodes," *J. Lightw. Technol.*, vol. 36, no. 17, pp. 3580–3585, Sep. 1, 2018.
- [15] S. Leclercq. *Discussion About Noise Equivalent Power and its Use for Photon Noise Calculation*. Accessed: Sep. 1, 2018. [Online]. Available: http://www.iram.fr/~leclercq/Reports/About_NEP_photon_noise.pdf
- [16] K. Karstad *et al.*, "Detection of mid-IR radiation by sum frequency generation for free space optical communication," *Opt. Lasers Eng.*, vol. 43, nos. 3–5, pp. 537–544, Mar. 2005.
- [17] Q. Zhou, K. Huang, H. Pan, E. Wu, and H. Zeng, "Ultrasensitive mid-infrared up-conversion imaging at few-photon level," *Appl. Phys. Lett.* vol. 102, no. 24, Jun. 2013, Art no. 241110.